

Study of mass transfer in viscoelastic liquids by segmented electrodiffusion velocity probes

V. SOBOLÍK

Institute of Chemical Process Fundamentals, Academy of Sciences of Czech Republic, CS-16502 Prague 6, Czech Republic

S. MARTEMYANOV

Institute of Electrochemistry, Russian Academy of Sciences, 117071 Moscow V-71, Russia

G. COGNET

Institute of Mechanics, BP 53 X, 38041 Grenoble Cedex, France

Received 15 May 1993; revised 19 August 1993

Mass transfer on a circular cylinder with a diameter of 0.52 mm was studied in polymer solutions by measuring the directional characteristics of a three-segment electrodiffusion velocity probe. The free stream velocity was varied in the range 0.01–0.31 m s⁻¹ and the polyacrylamide concentration in the range 0.001–1% (by mass). A small amount of polymer produced large changes in mass transfer distribution on the cylinder in comparison to the distribution in Newtonian liquid. In particular it has been shown that the transfer rate in the aft portion of the cylinder is greater than in the front part if the Weissenberg number exceeds some critical value. The situation was identified where the local mass transfer was constant around the cylinder, i.e. the surface was uniformly accessible to diffusion.

1. Introduction

Electrodiffusion sensors have been widely used for the quantitative measurements of wall shear stress and bulk velocity in Newtonian liquids [1–3]. For the measurement of both magnitude and direction of wall shear stress, segmented circular probes composed of two sensors separated by a thin insulating gap were designed [4, 5]. These probes allow unambiguous estimation of the flow direction in the range 0–180°. For measurements in the full range 0–360° three-segment circular probes were constructed [6]. With these probes it is also possible to estimate the normal velocity component close to the wall.

The three-segment wall shear stress probes were recently modified for velocity measurements [7]. As in triple-split hot film anemometric probes [8], the cylindrical surface of the electrodiffusion probes is divided into three equal electrochemically active segments. The probe is immersed into a depolarizer and the flow kinematics near the probe estimated from the limiting diffusion currents on the segments. For the flow of Newtonian liquid past a cylinder, the wall shear rate distribution has been obtained analytically [9] for Reynolds numbers smaller than one and numerically [10–12] for $1 < Re < 100$. This information is sufficient for the prediction of the total limiting current, and so-called directional characteris-

tics of the probe [7, 13, 14], by means of which the bulk velocity and flow direction can be estimated.

Electrodiffusion sensors have also been used in non-Newtonian liquids. Both the drag reduction in turbulent flow [15] and mass transfer on a thin cylindrical wire in dilute polymer solutions at very low Reynolds numbers [16] were studied. In spite of the fact that relatively simple electrodiffusion probes were used in the above mentioned experiments [16], it emerged that the mass transfer and hydrodynamical characteristics in the flow past a cylinder are strongly affected by the presence of a small quantity of polymer, even at very low Reynolds numbers. The measurements of the mean limiting current have shown considerable reduction (more than 50%) of global mass transfer rate on a cylinder in dilute polymer solutions in comparison with pure solvents. The region where global mass transfer rate was independent of the flow rate was found to be in good agreement with similar heat transfer experiments [17].

The measurements [16] of the instantaneous limiting diffusion current have shown that fluctuations exist in viscoelastic liquids even at small Reynolds numbers, for which no eddies occur behind the cylinder in Newtonian liquids. In other words a strong change in the character of hydrodynamic instabilities was found by the limiting diffusion current technique.

Hence electrodiffusion sensors are very sensitive for hydrodynamic measurements in dilute polymer solutions. It may be expected that fuller information about the hydrodynamic and mass transfer phenom-

This paper was presented at the International Workshop on Electrodiffusion Diagnostics of Flows held in Dourdan, France, May 1993.

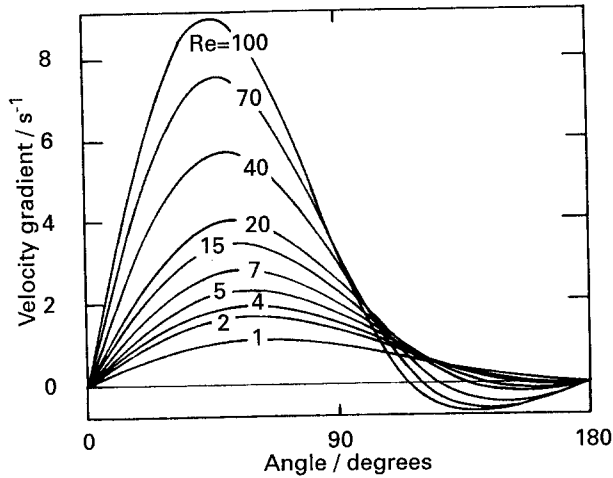


Fig. 1. Dependence of dimensionless velocity gradient B on angle ϕ .

ena in viscoelastic liquids can be obtained by using more sophisticated electrodiffusion probes, namely three-segment velocity probes [7].

In the present work directional characteristics of the three-segment electrodiffusion cylindrical probe are measured in solutions of polyacrylamide with different concentrations at various free stream velocities. The directional characteristics are analysed in order to obtain information about the mass transfer distribution and velocity field around a cylinder.

2. Hydrodynamics and mass transfer in flow past cylinder

To interpret the data obtained by the three-segment electrodiffusion velocity probe in polymer solutions, it is necessary to discuss the principle features of the flow and mass transfer around a cylinder.

Let v denote the free stream velocity, R the radius of the cylinder and ϕ the angle measured from the stagnation point. The velocity gradient distribution, $\gamma(\phi)$ can be then expressed by a series

$$B(\phi) = \sum_{n=1}^m b_n \sin(n\phi) \tag{1}$$

where B is the dimensionless velocity gradient, $B = \gamma R/v$. Illingworth [9] found an asymptotic solution with $m = 2$, which holds for Newtonian liquids and $Re < 1$. For medium Re , namely $1 < Re < 100$, numerical solutions exist [10–12] from which the velocity gradient can be expressed by the series (1) with three terms [14]. Velocity gradient distributions are shown in Fig. 1. According to the numerical solutions, separation of the boundary layer from the cylinder occurs at $Re = 5.8$. With increasing Re the separation point moves in the upstream direction, having the position $\phi = 118^\circ$ at $Re = 100$.

Equation 1 together with the well-known Lighthill formula[18], relating transfer rate at high Peclet number with the wall velocity gradient, allows prediction of the local diffusion flux distribution $j(\phi)$ [14]. Typical distributions of local Sherwood number, $Sh(\phi) = 2Rj(\phi)/Dc$, normalized by the Sherwood number at the stagnation point, $Sh(0)$, are given in Fig. 2.

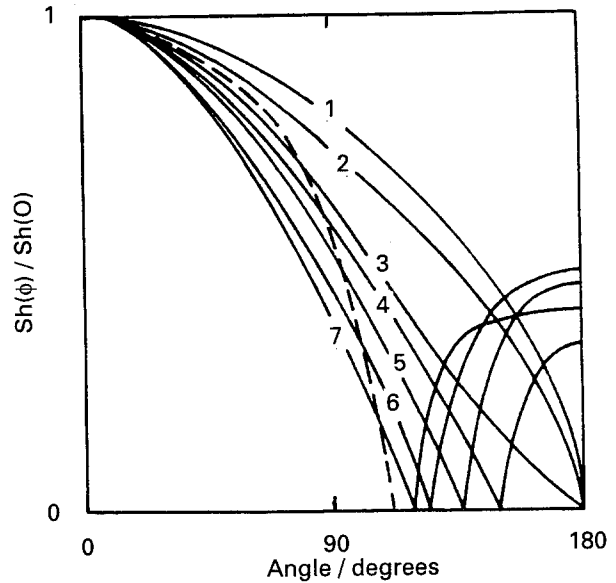


Fig. 2. Dependence of nromalized Sherwood number on angle ϕ . Dashed line corresponds to Sherwood number based on Blasius velocity distribution. Re : (1) 0.1, (2) 1, (3) 6, (4) 10, (5) 20, (6) 50 and (7) 100.

The velocity gradient is zero at the stagnation point and reaches maxima at ϕ of 90° and 53.1° for $Re \ll 1$ and $Re = 100$, respectively. For flow without separation the sign of the velocity gradient does not change and the local Sherwood number decreases monotonically. For flow with separation, both the velocity gradient and local Sherwood number are zero at the point of separation ϕ_0 . Moreover the sign of the velocity gradient changes and the local Sherwood number has discontinuous first derivative at the point of separation. It must be emphasized that, in Newtonian liquids, with or without separation, local Sherwood number reaches a maximum at the stagnation point.

Flow of non-Newtonian liquids past a cylinder has also received great attention [16, 17, 19–28]. The ratio of elastic and inertial forces is called the Weissenberg number

$$We = v\lambda/2R \tag{2}$$

The characteristic relaxation time, λ , depends on the structure and concentration of the polymer, as well as on the velocity gradient, and can be estimated by means of different methods [29].

Different effects were reported concerning the slow flow of viscoelastic liquids past a cylinder. Several authors observed drag reduction [21, 25] while an increase in drag was measured by others [17]. The theoretical analysis [22, 23] has indicated that, for lower values of We , the streamlines are shifted downstream in comparison to the Newtonian case. Drag reduction accompanies this effect. For higher values of We an upstream shift of the streamlines is predicted [19, 24] which leads to drag increase. The influence of the wall was studied by numerical simulation, flow visualization and drag measurements on a cylinder in an asymmetrical position with respect to the channel walls [27]. In contrast to Newtonian flow it was observed that streamlines in highly elastic

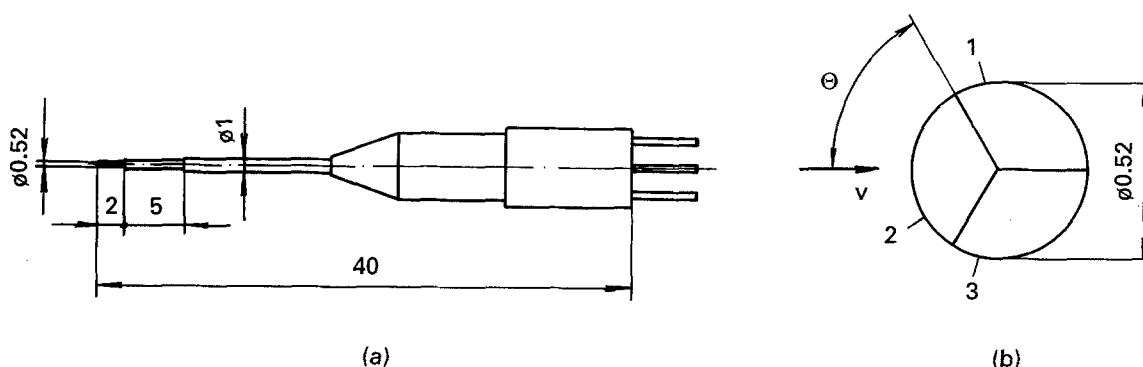


Fig. 3. Three-segment probe (a) and detailed cross-section (b) with definition of flow angle, Θ . Dimensions in millimetres.

liquids change dramatically with increasing velocity. The numerical analysis [27] has simulated qualitatively the effect of viscoelasticity on the force components but was unable to predict the observed changes in the streamline patterns.

The computer simulations of viscoelastic flow deal with rather low We because of the so-called high Weissenberg number problem, i.e. the finer the mesh the earlier in We the calculation fails. For example, flow past a sphere was solved for a maximum We of 4.5 [28]. Therefore it is not possible to predict the mass transfer on the cylinder in viscoelastic flow or to calculate directional characteristics of electrodiffusion three-segment velocity probes for high values of the Weissenberg number. However, it is possible to measure the directional characteristics and analyse them to get information about local mass transfer, from which the flow pattern can be estimated.

3. Experimental details

The electrodiffusion three-segment probe, see Fig. 3, was made by the procedure described in [7]. The active cylindrical surface with a diameter of 0.52 mm and a length of 2 mm was longitudinally split into three strips—working platinum electrodes which are denoted by the numbers 1, 2, 3.

The probe was immersed into a rotating vessel of liquid, see Fig. 4. The vessel had the form of an annulus for better manipulation and to economise on solution. The rotation speed was adjustable in the range 0.6–60 r.p.m. which corresponds to a free stream velocity of 0.01–1 m s⁻¹.

The mean time values of the currents from individual segments i_k ($k = 1, 2, 3$) were measured in solutions with different polymer concentrations and at different free stream velocities. The dependence of the normalized current, I_k , on the flow angle, Θ ,

$$I_k(\Theta) = i_k(\Theta) / \sum_{n=1}^3 i_n \quad (3)$$

is called the directional characteristic. The flow angle, Θ , is the angle between the free stream velocity and the line which separates the first and second segment, see Fig. 3. In other words directional characteristics denote normalized mass transfer rate on a segment with respect to the flow angle.

Measurements were made in water and aqueous solutions of polyacrylamide Separan AP 30. As the polymer was degraded rapidly by the commonly used depolarizer $K_3Fe(CN)_6$ and $K_4Fe(CN)_6$ with the supporting electrolyte K_2SO_4 , I_2 in a concentration of 0.038 M and KI in a concentration of 0.1 M were used. Solutions with different polymer concentrations were prepared by diluting a 1.33% solution of PAA by distilled water containing an appropriate amount of I_2 and KI. Despite the fact that the solutions were kept in closed glass bottles, the concentration of triiodine slowly decreased due to evaporation and sublimation. Thus the triiodine concentration was not exactly the same in all experiments. The other reason for the scatter of the total current may be the temperature, which changed over the range 17–24 °C. Because all measurements were done in the regime of the limiting diffusion current, variation

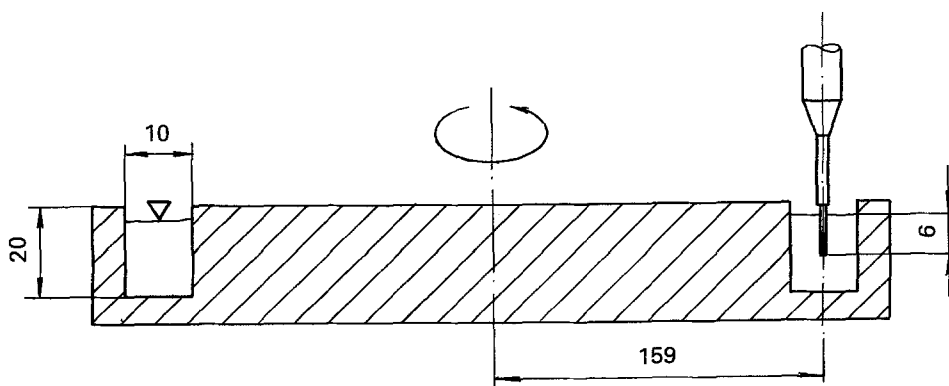


Fig. 4. Experimental setup. Dimensions in millimetres.

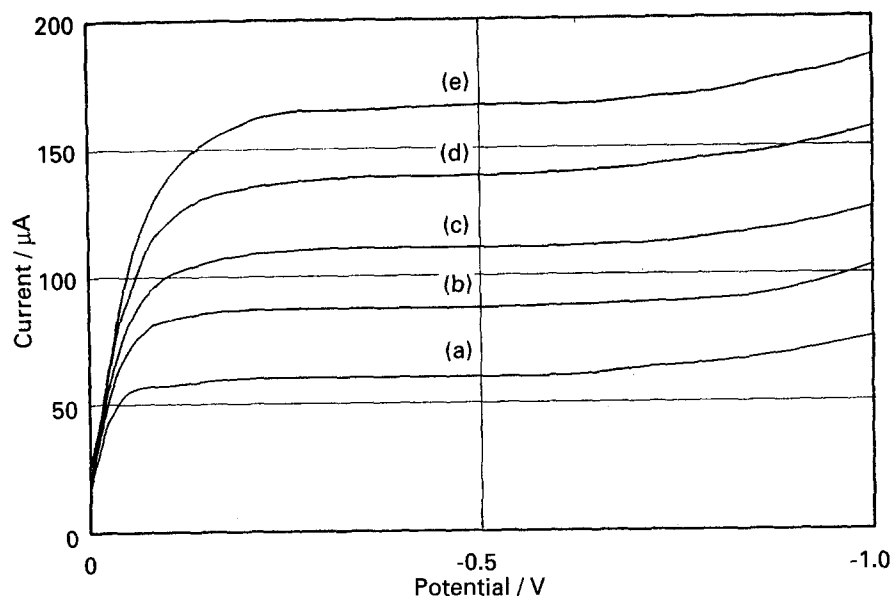


Fig. 5. Polarization curves in 1% PAA solution Free stream velocity: (a) 0.01 m s^{-1} , (b) 0.034 m s^{-1} , (c) 0.073 m s^{-1} , (d) 0.17 m s^{-1} , (e) 0.31 m s^{-1} .

of the triiodine concentration had no influence on the directional characteristics which represent relative values.

4. Results

The polarization curves are presented in Fig. 5 for 1% PAA solution at different flow rates. The character of the plateau confirms that the total current is controlled by the convective diffusion and hence the electrodiffusion technique can be applied in polymer solutions. The voltage between the working and auxiliary electrodes was adjusted to -0.6 V .

The typical directional characteristics measured in water and polymer solutions are shown in Fig. 6. In Newtonian liquids the mass transfer exhibits a maximum at the stagnation point. Therefore, the directional characteristics measured in water and solutions with lower polymer concentrations have maxima when the stagnation point is in the center of the relevant segment. For example, the angle $\Theta = 180^\circ$ corresponds to the position when the stagnation point is in the centre of the third segment.

The results presented in Fig. 6 show that a small amount of polymer changes the directional characteristics and hence the mass transfer rate on the segments. In comparison to Newtonian liquids, the directional characteristics measured in a dilute polymer, $c = 0.05\%$, at $v = 0.03 \text{ m s}^{-1}$ are much flatter. For a relatively high polymer concentration, $c = 0.5\%$, the directional characteristics become independent of the angle at $v = 0.01 \text{ m s}^{-1}$, see Fig. 6(c). Using the analogy with a rotating disc electrode, where the local mass transfer does not depend on the radius, the cylindrical surface of the probe is uniformly accessible. In a concentrated polymer, $c = 1\%$, the directional characteristic of the third segment reaches its maximum at $\Theta = 0^\circ$ and minimum at $\Theta = 180^\circ$, see Fig. 6(d). This means, that the mass transfer in the vicinity of the rear critical point is greater than at the stagnation point.

The directional characteristics measured at a given velocity and concentration are similar curves shifted about 120° . This means that each of the three probe segments gives practically the same mass transfer rate. Thus only one directional characteristic, namely the third segment is considered in the following. The symmetry of the directional characteristics gives proof of regular probe geometry and good accuracy of the measurements.

The influence of polymer concentration on the mass transfer is shown in Fig. 7, where the directional characteristics of the third segment are depicted at different velocities. It is evident that the ratio of the mass transfer rate in the vicinity of the rear critical point to that in the vicinity of the stagnation point increases with increasing polymer concentration and free stream velocity. This ratio is even greater than that for polymer concentrations 0.5 and 1% at a velocity greater than 0.01 m s^{-1} .

Due to the difficulties with the triiodine concentration and temperature control mentioned in the experimental part, only qualitative conclusions on the influence of the polymer concentration on the total current can be made. In agreement with the experimental data [16, 17] we have found, that the total current in polymer solution is smaller than in Newtonian liquid at the same free stream velocity. However, the dependence of the total current on polymer concentration exhibits a minimum at a concentration between 0.01 and 0.05%. Nevertheless, dependence on the total current on polymer concentration will be studied in greater detail.

5. Discussion and conclusions

The directional characteristics measured by the three-segment velocity probe have shown large changes in the mass transfer distribution on the cylinder in polymer solutions in comparison with Newtonian liquid. At a velocity of 0.071 m s^{-1} the directional character-

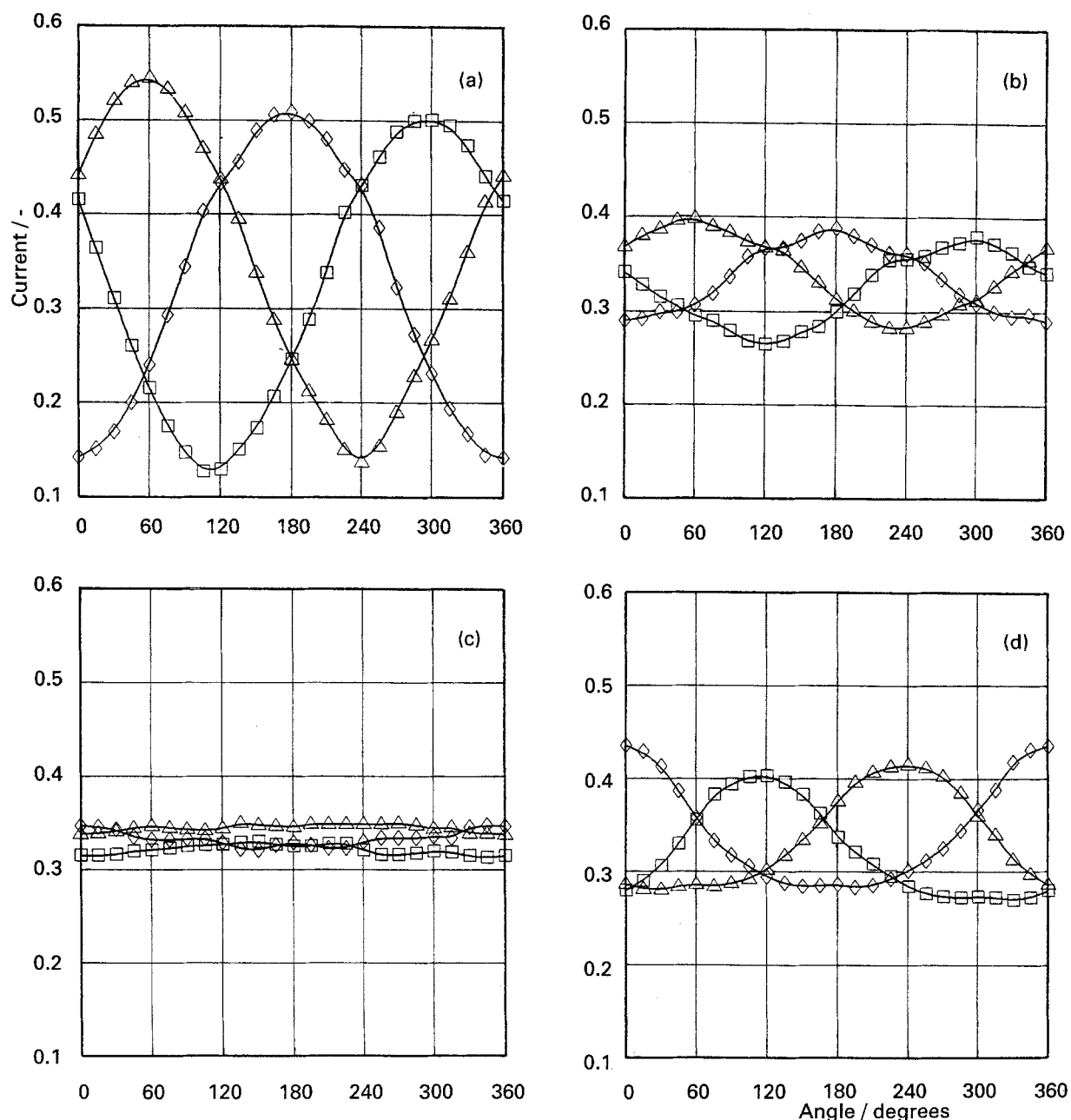


Fig. 6. Directional characteristics (a) $c = 0$, $v = 0.034 \text{ m s}^{-1}$; (b) $c = 0.05\%$ PAA, $v = 0.034 \text{ m s}^{-1}$; (c) $c = 0.5\%$ PAA, $v = 0.01 \text{ m s}^{-1}$; (d) $c = 1\%$ PAA, $v = 0.034 \text{ m s}^{-1}$. Segment number: (\square) 1, (\triangle) 2, (\diamond) 3.

istics are flatter even at such small polymer concentration as 0.001%. In contrast to the Newtonian liquid, the mass transfer rate in the front portion of the cylinder is smaller than in the aft portion in polymers with concentrations of 0.5 and 1% at velocities greater than 0.01 m s^{-1} .

Under certain constraints, the product of free stream velocity and polymer concentration is proportional to the Weissenberg number. The experiments have shown that the transfer rate on the aft portion of the cylinder is greater than on the front part if the Weissenberg number exceeds some critical value. The critical Weissenberg number, estimated by means of the polymer relaxation time given by Bowersdorff [30], is equal to 5. This value should be considered as a first estimation only.

In Newtonian flow with separation the ratio of the mass transfer rate on the aft to front cylinder portions

increases with increasing Re due to back flow between the rear critical and separation point. The back flow cannot explain the phenomena observed in the polymer solutions. Indeed, the transition from the 'Newtonian' character of the mass transfer to the 'anomaly' one (mass transfer rate on the rear cylinder portion is greater than on the front one) passes through the situation where the cylinder surface is uniformly accessible in the diffusion sense. It is obvious, that the uniformly accessible surface, $Sh(\Theta) = \text{const}$, cannot exist in flow where separation takes place, because the Sherwood number is zero at the separation point. It seems that the upstream shift of streamlines, described in [19], dominates in our experiments especially at higher Weissenberg numbers. In this case the stagnation, or slow velocity, layer formed in the front part of the cylinder results in a smaller mass transfer rate. The upstream shift of

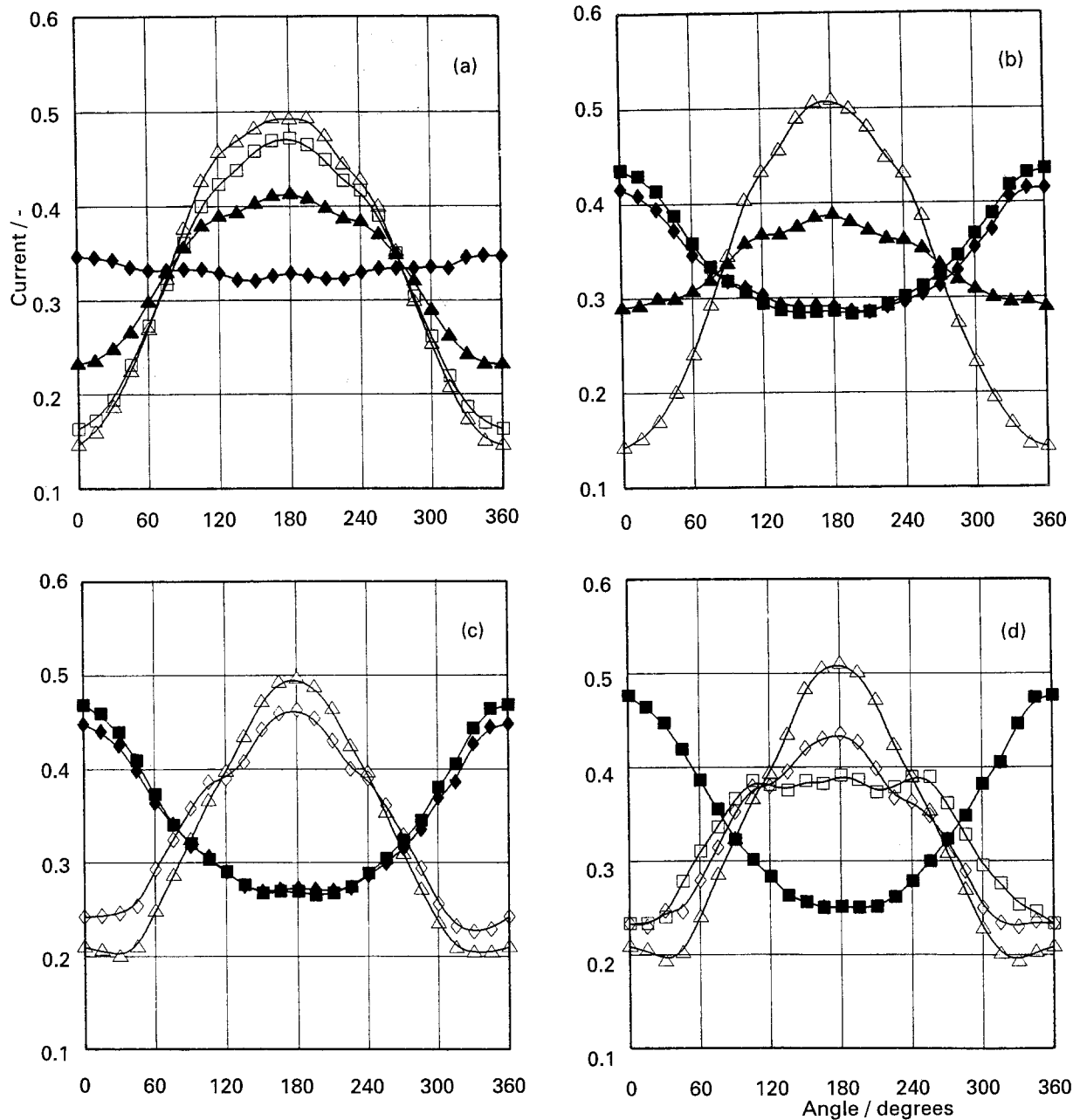


Fig. 7. Influence of polymer concentration on the mass transfer on the third segment. Velocity: (a) 0.01, (b) 0.034, (c) 0.17, (d) 0.31 m s⁻¹. Polymer concentration: (△) 0%, (◇) 0.001%, (□) 0.01%, (▲) 0.05%, (◆) 0.5%, (■) 1%.

streamlines can stabilize the flow past the cylinder and prevent flow separation. It should be noted that no flow separation was detected by visualization [19].

In comparison with the traditional experimental techniques, i.e. flow visualization and drag and overall heat or mass transfer measurement, the three-segment electrodiffusion velocity probes give additional information about the mass transfer distribution. As the diameter of this probe is small, flows with high Weissenberg numbers can be realized.

Acknowledgements

This work was done in the laboratory LEGI of the Institute of Mechanics, Grenoble. The authors express their thanks to the Rhone-Alpes region and the Ministry of Education of France which made this work possible by a grant TEMPRA (V.S.) and a

PAST position (S.M.), respectively. The contribution of Dr O Wein to the development of the software is greatly appreciated.

References

- [1] T. J. Hanratty and J. A. Campbell, 'Measurement of wall shear stress' in 'Fluid mechanics measurements' (edited by R.J. Goldstein), Hemisphere, Washington (1983).
- [2] V. E. Nakoryakov, A. P. Burdukov, O. N. Kashinsky and P. I. Geshev, 'Electrodiffusion method of investigation into the local structure of turbulent flows' (edited by V. G. Gasenko), Institute of Thermophysics, Novosibirsk (1986) (in Russian).
- [3] B. M. Grafov, S. A. Martemyanov and L. N. Nekrasov, 'The turbulent diffusion layer in electrochemical systems', Nauka, Moscow (1990) (in Russian).
- [4] B. Py and J. Gosse, *C.R. Acad. Sc. Paris* **269A** (1969) 401.
- [5] C. Deslouis, F. Huet, O. Gil and B. Tribollet, *Experiments in Fluids*, in press.
- [6] V. Sobolík, O. Wein, O. Gil and B. Tribollet, *ibid.* **9** (1990) 43.

- [7] V. Sobolík, J. Pauli and U. Onken, *ibid* **11** (1991) 186.
- [8] F. E. Jorgensen, *DISA Information* **27** (Jan. 1982) 15.
- [9] C. R. Illingworth, 'Flow at small Reynolds number' in 'Laminar boundary layers' (edited by L. Rosenhead), Clarendon Press, Oxford (1963).
- [10] H. B. Keller and H. Takami, 'Numerical studies of steady viscous flow about cylinders' in 'Numerical Solutions of Nonlinear Differential Equations' (edited by D. Greenspan), Prentice-Hall, Englewood Cliffs, NJ (1966).
- [11] A. C. Hamielec and J. D. Raal, *Phys. Fluids* **12** (1969) 11.
- [12] S. C. R. Dennis and G.-Z. Chang, *J. Fluid Mech.* **42** (1970) 471.
- [13] O. Wein and V. Sobolík, *Coll. Czech. Chem. Commun.* **52** (1986) 2169.
- [14] V. Sobolík and O. Wein, *Int. J. Heat Mass Transf.* **34** (1991) 1929.
- [15] A. McConaghy and T. J. Hanratty, *AIChE J.* **23** (1977) 493.
- [16] A. Ambari, C. Deslouis and B. Tribollet, *Chem. Eng. Commun.* **29** (1984) 63.
- [17] D. F. James and A. J. Acosta, *J. Fluid Mech.* **42** (1970) 269.
- [18] M. J. Lighthill, *Proc. Roy. Soc., Lond.* **A202** (1950) 359.
- [19] J. S. Ultman and M. M. Denn, *Chem. Eng. J.* **2** (1971) 81.
- [20] E. Zana, G. Tiefenbruch and L. G. Leal, *Rheol. Acta* **14** (1975) 891.
- [21] R. P. Chhabra, P. H. Uhlherr and D. V. Boger, *J. Non-Newton. Fluid Mech.* **6** (1980) 187.
- [22] P. Townsend, *ibid.* **6** (1980) 219.
- [23] F. Sugeng and R. I. Tanner, *ibid.* **20** (1986) 281.
- [24] D. Sigli and M. Coutanceau, *ibid.* **2** (1977) 1.
- [25] B. Mena, O. Manero and L. G. Leal, *ibid.* **26** (1987) 247.
- [26] M. D. Chilcott and J. M. Rallison, *ibid.* **29** (1988) 381.
- [27] S. A. Dahir and K. Walters, *J. Rheology* **33** (1989) 781.
- [28] H. Jin, N. Phan-Thien N and R. I. Tanner, *Comput. Mech.* **8** (1991) 409.
- [29] R. B. Bird, R. C. Armstrong and O. Hassager, 'Dynamics of polymeric liquids'. Vol. 1. 'Fluid Mechanics', J. Wiley & Sons, New York (1977).
- [30] H. W. Bewersdorff, *Rheol. Acta* **23** (1984) 538.